SMC-TR-05-17

AEROSPACE REPORT NO.
TR-2005(8555)-5

Low-Temperature Failure Mode for Nickel-Hydrogen Cells

5 August 2005

Prepared by

A. H. ZIMMERMAN
Electronics and Photonics Laboratory
Laboratory Operations

Prepared for

SPACE AND MISSILE SYSTEMS CENTER
AIR FORCE SPACE COMMAND
2430 E. El Segundo Boulevard
Los Angeles Air Force Base, CA 90245

Engineering and Technology Group

THE AEROSPACE CORPORATION
El Segundo, California

This report was submitted by The Aerospace Corporation, El Segundo, CA 90245-4691, under Contract No. FA8802-04-C-0001 with the Space and Missile Systems Center, 2430 E. El Segundo Blvd., Los Angeles Air Force Base, CA 90245. It was reviewed and approved for The Aerospace Corporation by B. Jaduszliwer, Principal Director, Electronics and Photonics Laboratory. Michael Zambrana was the project officer for the Mission-Oriented Investigation and Experimentation (MOIE) program.

This report has been reviewed by the Public Affairs Office (PAS) and is releasable to the National Technical Information Service (NTIS). At NTIS, it will be available to the general public, including foreign nationals.

This technical report has been reviewed and is approved for publication. Publication of this report does not constitute Air Force approval of the report's findings or conclusions. It is published only for the exchange and stimulation of ideas.

Michael Zambrana
SMC/AXE

REPORT DOCUMENTATION PAGE

Form Approved
OMB No. 0704-0188

1. REPORT DATE (*DD-MM-YYYY*)	2. REPORT TYPE	3. DATES COVERED (*From - To*)
05-07-2005		

4. TITLE AND SUBTITLE

Low-Temperature Failure Mode for Nickel-Hydrogen Cells

5a. CONTRACT NUMBER
FA8802-04-C-0001

5b. GRANT NUMBER

5c. PROGRAM ELEMENT NUMBER

6. AUTHOR(S)

A. H. Zimmerman

5d. PROJECT NUMBER

5e. TASK NUMBER

5f. WORK UNIT NUMBER

7. PERFORMING ORGANIZATION NAME(S) AND ADDRESS(ES)

The Aerospace Corporation
Laboratory Operations
El Segundo, CA 90245-4691

8. PERFORMING ORGANIZATION REPORT NUMBER

TR-2005(8555)-5

9. SPONSORING / MONITORING AGENCY NAME(S) AND ADDRESS(ES)

Space and Missile Systems Center
Air Force Space Command
2450 E. El Segundo Blvd.
Los Angeles Air Force Base, CA 90245

10. SPONSOR/MONITOR'S ACRONYM(S)
SMC

11. SPONSOR/MONITOR'S REPORT NUMBER(S)
SMC-TR-05-17

12. DISTRIBUTION/AVAILABILITY STATEMENT

Approved for public release; distribution unlimited.

13. SUPPLEMENTARY NOTES

14. ABSTRACT

A mechanism has been proposed that can potentially lead to rapid degradation and failure of nickel-hydrogen cells as a result of electrolyte freezing. It has been shown that there are chemical processes that can occur within the operating nickel-hydrogen cell that can raise the electrolyte freezing point in some cell designs up to the –5 to –10°C operational temperature range that cells can experience in some applications. The model that describes this failure mode suggests that the operational conditions where this failure mode is most likely to be seen is during long-term trickle charge at cold temperatures. It is recommended that nickel-hydrogen cell designs that are required to operate at temperatures well below 0°C should be evaluated for long-term degradation 10°C below their lowest expected operating temperature during extended trickle charge. This will assure that there is sufficient temperature margin to accommodate thermal variability between the individual cells in a battery power system.

15. SUBJECT TERMS

Nickel-hydrogen cell, Battery failure modes, Electrolyte freezing

16. SECURITY CLASSIFICATION OF:			17. LIMITATION OF ABSTRACT	18. NUMBER OF PAGES	19a. NAME OF RESPONSIBLE PERSON
					A. H. Zimmerman
a. REPORT	b. ABSTRACT	c. THIS PAGE			19b. TELEPHONE NUMBER (*include area code*)
UNCLASSIFIED	UNCLASSIFIED	UNCLASSIFIED		19	(310)336-7415

Contents

Figures

1. Introduction

The performance of nickel-hydrogen battery cells at low temperatures is generally thought to be ultimately limited by the temperature where the KOH electrolyte used in these cells freezes. If the electrolyte freezes, it is expected to create a high resistance and cut off the flow of the reagents needed by the nickel and hydrogen electrodes for operation. Here we present modeling analyses that examine the expected freezing point of the electrolyte in nickel-hydrogen cells of different designs, under the actual operating conditions of the cells. These models consider the effects of cell chemical and transport processes on the KOH concentration in the electrodes during operation and the changes in the freezing point of the electrolyte that are possible.

The nickel-hydrogen cell designs in common use today use either 26 or 31 weight % KOH electrolyte to fill the cells when they are activated. Once the cells are sealed with these electrolyte concentrations, it has customarily been believed that electrolyte freezing would not become a concern until the cell temperature approached the freezing point of the electrolyte. The freezing points are –42°C for 26% KOH, and –61°C for 31% KOH. Since these temperatures are quite low relative to the lowest operating temperatures considered for nickel-hydrogen cells, which is in the range of –10 to –15°C, concerns about electrolyte freezing are generally minimal. Here we report analyses that suggest that there are normal operational conditions for nickel-hydrogen cells that can result in unexpected electrolyte freezing, and that that freezing may hasten failure of the cell.

2. Analysis

2.1 Cell Chemistry

Several factors can influence the concentration of KOH electrolyte within an operating nickel-hydrogen cell and make that concentration different from that put into the cell when it was activated. The first of these factors is the production and consumption of hydroxide and water at the electrodes as they are charged and discharged. During recharge, water is produced, and hydroxide ions are consumed in the nickel electrodes, which will reduce the local electrolyte concentration in the nickel electrode, as indicated by Eq. (1). During discharge, the opposite processes occur to give a more concentrated electrolyte in the nickel electrode.

$$Ni(OH)_2 + OH^- \xrightarrow{Recharge} NiOOH + H_2O + e^- \quad (1)$$

During discharge at the hydrogen electrode, similar production and consumption of reagents result in a decrease in the local electrolyte concentration in the hydrogen electrode, as indicated by Eq. (2). During recharge, the electrolyte will become more concentrated in the hydrogen electrode by the process of generating hydrogen gas.

$$H_2 + 2OH^- \xrightarrow{Discharge} 2H_2O + 2e^- \quad (2)$$

The gradient that is set up between the nickel and the hydrogen electrode by the charge and discharge reactions will tend to be dissipated by diffusion of ions through the separator at a rate proportional to the magnitude of the concentration gradient. The cell will continue to work well as long as the diffusional current can match the cell current without requiring an excessive concentration gradient between the electrodes. If diffusion is not fast enough, the cell displays "diffusion limited" behavior, meaning that its voltage will drop precipitously during discharge, or rise precipitously during recharge.

An additional recharge reaction that can influence the electrolyte concentration is the formation of γ-NiOOH from β-NiOOH at high states of charge and when a cell is in overcharge. The γ-NiOOH phase structure incorporates one KOH molecule for every three nickel lattice sites, as indicated by Eq. (3). The reaction indicated by Eq. (3) is not reversible since there is no evidence that the γ-NiOOH phase (which is chemical shorthand for $NiOOH(NiO_2)_2 \bullet KOH$) can undergo electrochemical discharge by the reverse of Eq. (3) to reform the less stable β-NiOOH phase.

$$3\beta - NiOOH + 2OH^- + KOH \xrightarrow{Charge} NiOOH(NiO_2)_2 \bullet KOH + 2H_2O + 2e^- \quad (3)$$

The γ-NiOOH phase is interesting because it is more difficult to form than the β-NiOOH that normally does most of the charge and discharge cycling in the nickel electrode, but it is also the most stable material in the nickel electrode once it is formed. This means that it has a lower discharge voltage, and will typically be the last material in the electrodes to be discharged. The γ-NiOOH phase discharges to an α-$Ni(OH)_2$ phase that will lose its potassium, after which it will recrystallize back to the β-$Ni(OH)_2$ phase if it is not recharged immediately back to the γ-NiOOH phase. This process is indicated by Eq. (4).

$$NiOOH(NiO_2)_2 \bullet KOH + 5H_2O + 5e^- \xrightarrow{\text{Discharge}} 3\alpha Ni(OH)_2 + KOH + 5OH^- \qquad (4)$$

A significant consequence of the reactions in Eqs. (3) and (4) is that the active material in the nickel electrode can chemically tie up a significant amount of the KOH that is in the electrolyte if a large portion of the active material is converted into the γ-NiOOH phase. The γ-NiOOH phase formation is favored by higher KOH concentration, by lower temperatures, by higher recharge/overcharge rates, and by higher cobalt additive levels in the nickel electrode active material. Typically, any active material that is charged in a nickel electrode and that has not been discharged in a long period of time will be present as the more stable γ-NiOOH phase. Therefore, this tends to include the nickel precharge that is built into nickel-hydrogen cells by most manufacturers.

2.2 Analysis of γ-NiOOH Effects on Electrolyte

The KOH electrolyte used in nickel-hydrogen cells exhibits a freezing point that depends on KOH concentration as indicated in Figure 1. Because Eq. (3) tells us that each nickel atom that converts

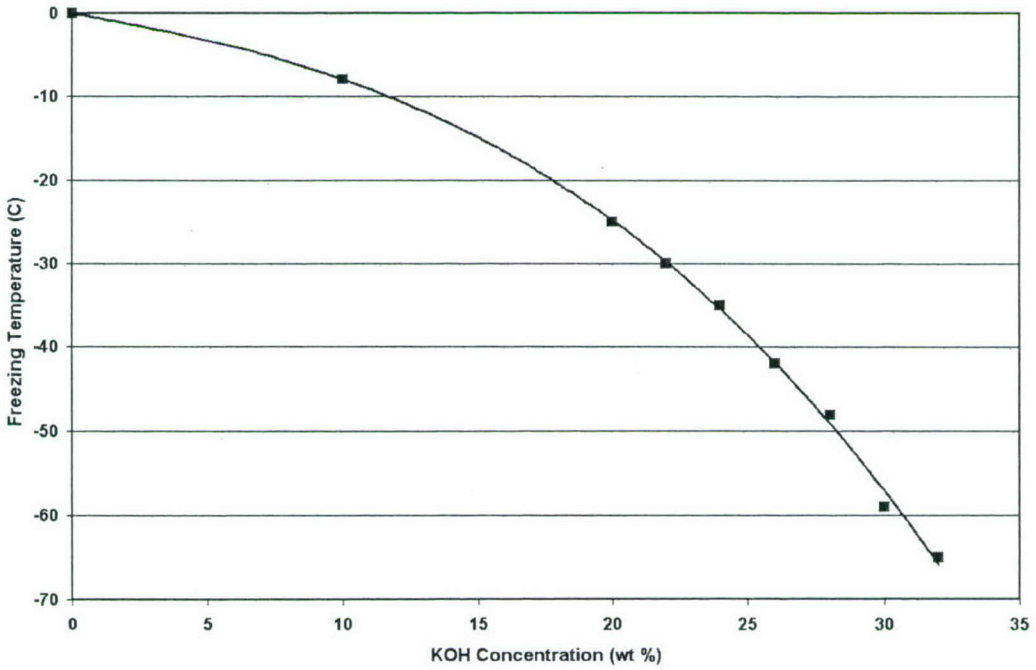

Figure 1. Freezing point of KOH electrolyte as a function of concentration.

into the γ-NiOOH phase will absorb ⅓ of a KOH molecule, we may calculate the effect of varying amounts of γ-NiOOH formation on the concentration of the electrolyte, and thus on the freezing point of the electrolyte. The starting point for this calculation is the initial KOH concentration with no γ-NiOOH phase formed, and the amount KOH present in the nickel-hydrogen cell in terms of g/Ah.

As an example, this computation has been performed for a cell that started with 26% KOH electrolyte at a level of 3.0 g/Ah, which is typical of some nickel-hydrogen cell designs. The results are shown in Figure 2, where the expected KOH concentration, as well as its freezing point, is indicated as a function of the amount of γ-NiOOH.

The result of Figure 2 indicates that the formation of a sufficient amount of γ-NiOOH in a cell having 3g/Ah of 26% KOH can result in a dramatic lowering of the electrolyte concentration, and an increase in the freezing point of the electrolyte from about –42°C up to nearly –2°C in the extreme case where all the active material is converted to γ-NiOOH. However, the results in Figure 2 do not tell us under what conditions of cell operation it may be possible to form large amounts of γ-NiOOH, how rapidly this material can form, or whether, in fact, it is at all possible to convert large amounts of active material into the γ-NiOOH phase in real nickel-hydrogen cells.

The sensitivity of the freezing point of the electrolyte to the amount of 26% electrolyte in the cell and amount of γ-NiOOH formed can be examined using the results in Figure 3. At each of the four temperatures in Figure 3, the amount of γ-NiOOH that has to form to initiate freezing is plotted as a function of the amount of electrolyte in the cell. At each temperature, the point where it takes 100%

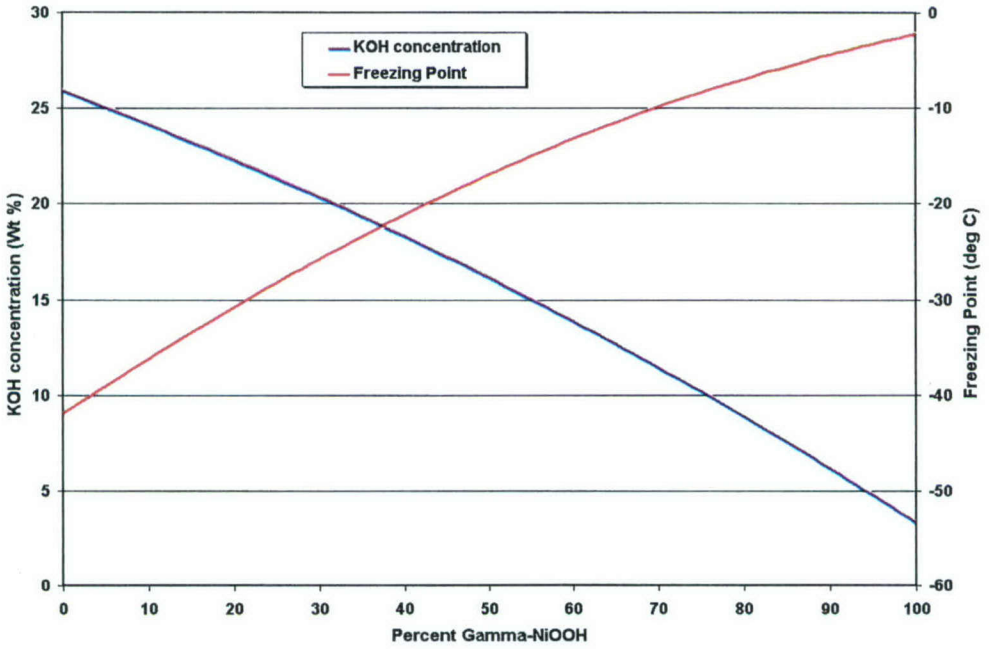

Figure 2. KOH concentration expected for different amounts of γ-NiOOH formation in a nickel-hydrogen cell initially having 3.0g/Ah of 26% KOH electrolyte. The freezing point of the KOH at each point is also indicated, based on the freezing point curve of Figure 1.

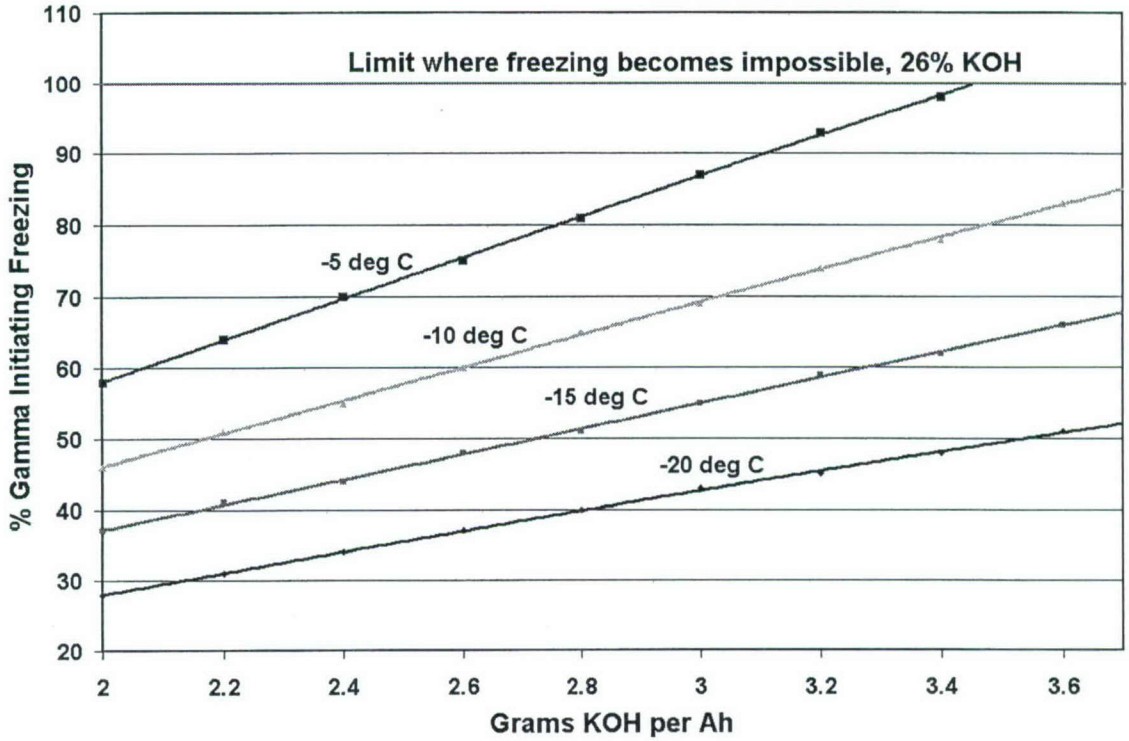

Figure 3. Amount of γ-NiOOH than can form before the electrolyte freezes at various temperatures, as a function of the electrolyte fill in the cell in grams of KOH per Ah of cell capacity. The initial electrolyte concentration is 26%.

γ-NiOOH to initiate freezing indicates the amount of 26% electrolyte that is required to prevent freezing for any amount of γ-NiOOH possible. The results in Figure 3 show that for 26% KOH, quite high levels of electrolyte are needed in a cell to preclude any possibility of electrolyte freezing, even at temperatures as high as –5°C. Typical electrolyte fill levels in cells with 26% KOH electrolyte are 2.8 to 3.0 g/Ah.

A similar sensitivity analysis can be performed for a cell design using 31% KOH electrolyte, providing the results shown in Figure 4. In this case, there appears to be a relatively wide range of temperatures where it is not possible to freeze the electrolyte even if the amount of γ-NiOOH formed reaches 100% for the typical electrolyte fill levels of about 3.5 g/Ah used in many such cell designs. Figure 4 indicates that with a 3.5-g/Ah quantity of electrolyte, the cell can be operated down to nearly –15°C without any possibility of freezing the electrolyte. However, one must keep in mind that with 31% KOH it is easier to form large amounts of γ-NiOOH, making it more likely that 31% KOH cells will actually operate at the higher γ-NiOOH levels than will 26% KOH cells.

Experience with nickel-hydrogen cells indicates that it is possible to significantly increase the amount of capacity of a nickel-hydrogen cell by operating it at low temperatures. Operation at temperatures as low as –10°C has been frequently used in recent years to take advantage of this significant capacity gain. The only known mechanism in the nickel-hydrogen cell that provides this capacity gain at reduced temperatures involves the formation of significant quantities of γ-NiOOH. The analyses of Figures 2 through 4 suggests that operating nickel-hydrogen cells at low temperatures to reap the

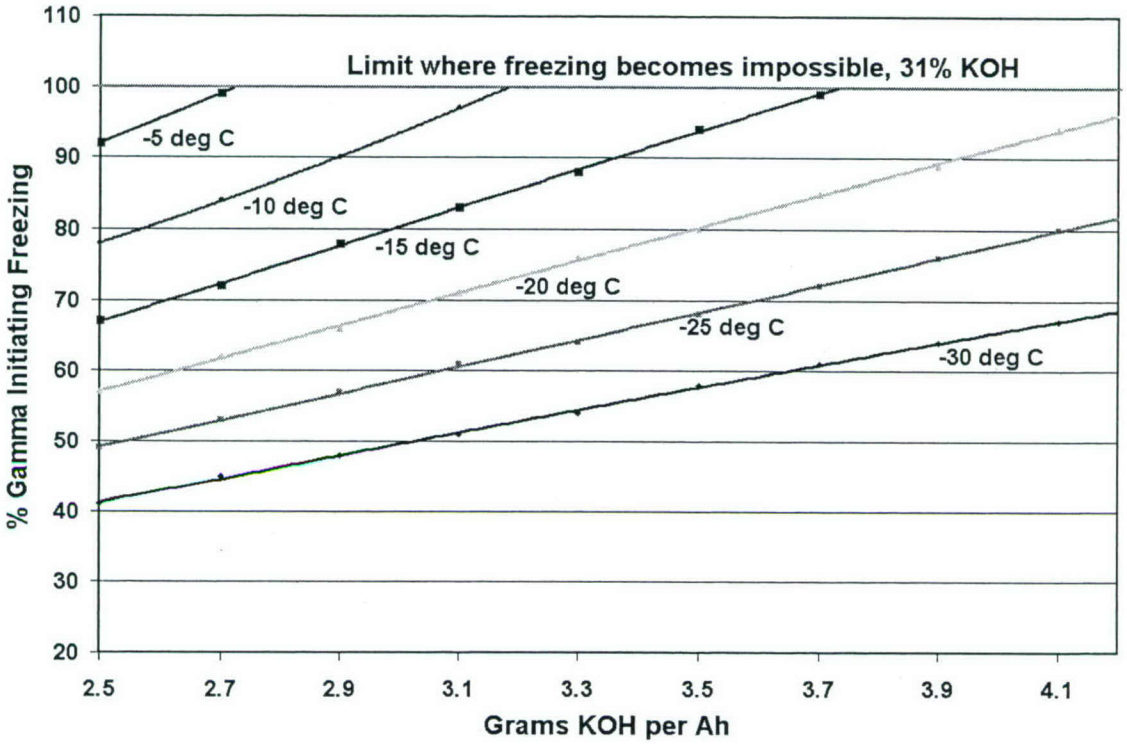

Figure 4. Amount of γ-NiOOH than can form before the electrolyte freezes at various temperatures, as a function of the electrolyte fill in the cell in grams of KOH per Ah of cell capacity. The initial electrolyte concentration is 31%.

benefits of increased capacity can significantly decrease the margin between where the cell operates and the freezing point of the electrolyte. In fact, these results suggest that there is a significant range of chemical conditions internal to many commonly used nickel-hydrogen cell designs that could result in electrolyte freezing for realistic cell thermal environments.

The key question that must be asked is: Under what conditions of cell operation can γ-NiOOH levels high enough to cause electrolyte freezing to be encountered, and how rapidly can these levels form in cells?

3. Nickel-hydrogen Cell Modeling

A sufficiently realistic nickel-hydrogen model can provide a reasonable indication of the rate of γ-NiOOH formation and the level of γ-NiOOH produced under typical conditions of cell operation. This type of a model can thus provide the rate at which the KOH concentration changes and the limit that the KOH concentration will be expected to reach after periods of recharge or trickle charge at various temperatures. A model has been developed at The Aerospace Corporation[1] that is capable of simulating nickel-hydrogen cell voltage and capacity performance with an accuracy that is comparable to the reproducibility of repeated measurements on different cells of a given design. This model is based on a first principles simulation of all processes known to occur in nickel-hydrogen cells, and utilizes a finite-element computer construct of the cell that can have an arbitrarily realistic geometry, as well as a realistic microstructure for the porous electrodes. This model has been validated based on cell-level data over the temperature range of 0–20°C, and thus its accuracy at sub-zero temperatures may be uncertain. However, the model realistically predicts the observed increase in cell capacity that accompanies the formation of γ-NiOOH at lower temperatures in the range where it has been validated.

This model provides results that are dependent on the thermal environment of the nickel-hydrogen cell. Since thermal environments are specific to each case of cell operation, we will run model simulations using isothermal conditions for the purposes of a sensitivity analysis. The model results are likely to differ from those of an actual cell since real cells generate heat and are exposed to external thermal sources and sinks, and therefore will have some thermal gradients through the electrode stack. To parameterize the effects of temperature, this isothermal model was run at temperatures from –20°C to +10°C.

The geometric cell model that has been chosen for these studies is a very simple one consisting of a nickel electrode that is in contact with a separator and a hydrogen electrode. The backside of the hydrogen electrode has a gas screen that is in contact with a gas space. The gas space is sized to give about a 900-psia maximum pressure when the cell is charged at 10°C for 16 h at a C/10 rate. The nickel electrode uses a realistic distribution of active material at a loading level of 1.65–1.70g/cc void volume. The active material is distributed realistically relative to the sinter as shown in Figure 5, where the white regions correspond to nickel sinter and the black regions are uniformly filled with active material.

Two different models were run. The first model used an electrolyte concentration of 26%, and had 3.0 g/Ah of electrolyte with single layer Zircar separator. The nickel electrodes contained 10% cobalt and 84% porous dry sinter substrate, and were loaded to 1.65 g/cc void volume. The second model used an electrolyte concentration of 31% and had 3.5 g/Ah of electrolyte with double layer Zircar separator. In the second model, the nickel electrodes contained 5% cobalt and 80% porous slurry sinter substrate, and were loaded to 1.70-g/cc void volume.

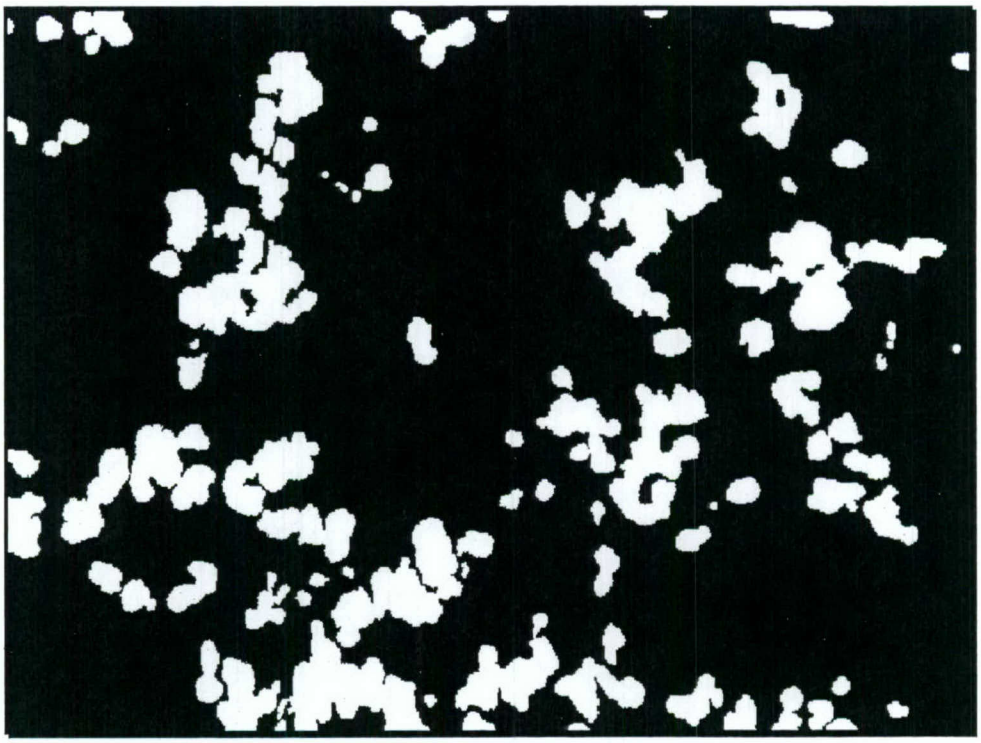

Figure 5. Nickel electrode microstructure used to model cell behavior. The white regions are nickel metal and black regions active material. The image corresponds to a 60 by 40 μm cross-sectional region of the nickel electrode.

Each of these models was run through an electrical simulation that was intended to examine the long-term buildup of γ-NiOOH during trickle charge, particularly at reduced operating temperatures. Each electrical simulation involved charge at C/10 for 16 h, discharge at C/2 to 1.0 V, recharge at C/10 for 16 h, and then trickle charge for two weeks at rates of C/50, C/100, and C/200.

3.1 Model Results with 26% KOH Electrolyte

The results from the simulations done with the cell containing 3.0 g/Ah of 26% KOH electrolyte are summarized in Figures 6 through 8. Figure 6 shows the change in cell electrolyte concentration during the two cycles and the two-week trickle charge period when a C/100 trickle charge rate was used. For this model, complete conversion of all the active material into γ-NiOOH leaves the electrolyte at about a 4% concentration. At the higher temperatures, it is significantly more difficult to form γ-NiOOH; thus the KOH concentration stabilizes at a level well above 4%. As the temperature is reduced to –10°C, it becomes possible to convert most of the active material to γ-NiOOH.

During the trickle charge period, less than a 0.1% concentration gradient was sustained between the nickel electrode and the hydrogen electrode at 10°C. At the end of the C/10 recharge, the concentration gradient between the electrodes was significantly greater. This observed concentration gradient at the end of the C/10 recharge and during the C/100 trickle charge are plotted in Figure 7. The concentration gradients increase as temperature falls, until at about –12°C, where the cell stops working in the model due to an inadequate diffusion rate.

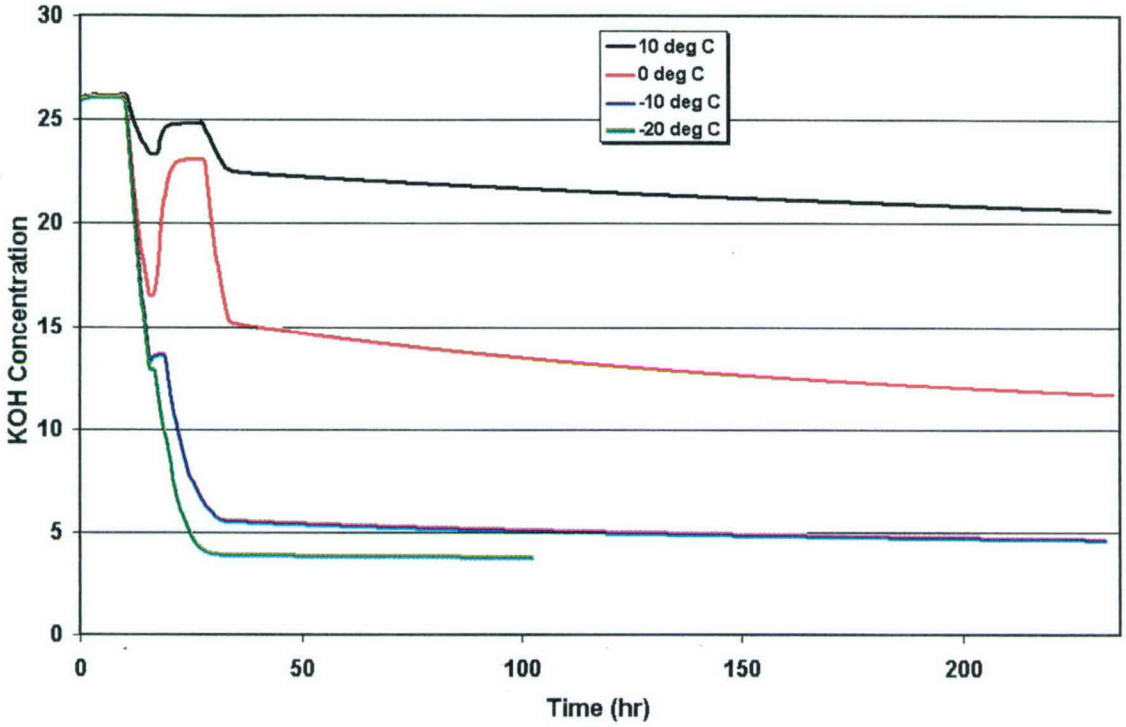

Figure 6. Concentration changes during simulations of a model cell initially containing 26% KOH, using a C/100 trickle charge rate. The concentration limit reached at about 4% corresponds to complete conversion of the active material to γ-NiOOH.

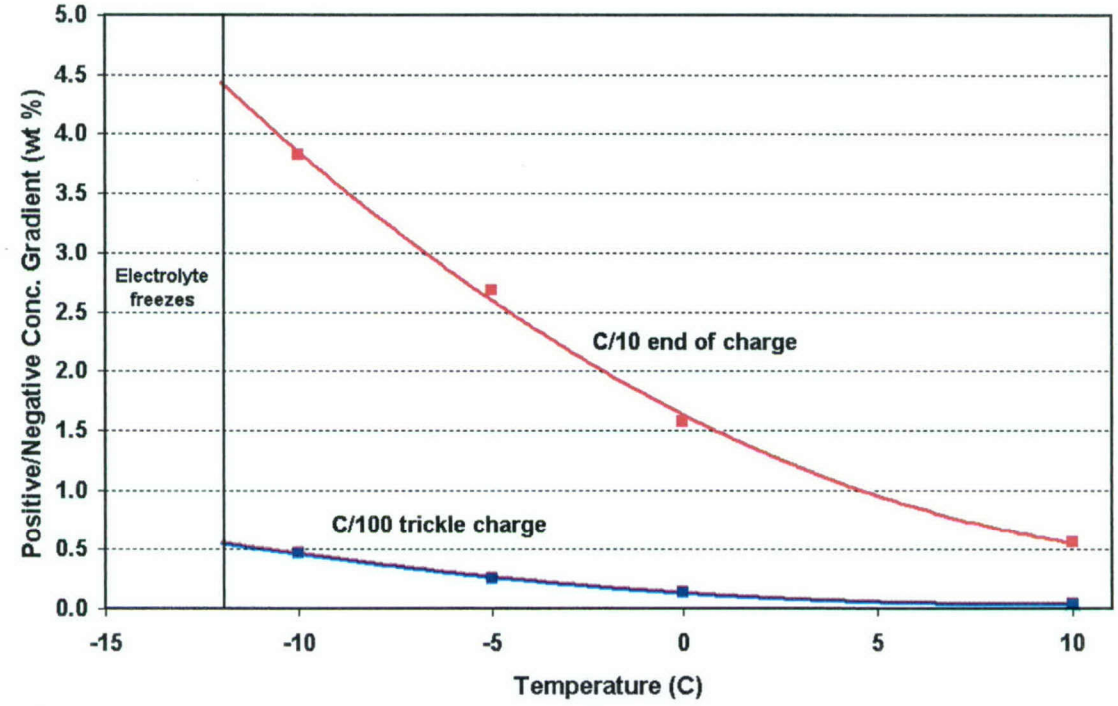

Figure 7. Worst-case electrolyte concentration gradient developed between the nickel and the hydrogen electrodes as a function of operating temperature, initially with 26% KOH.

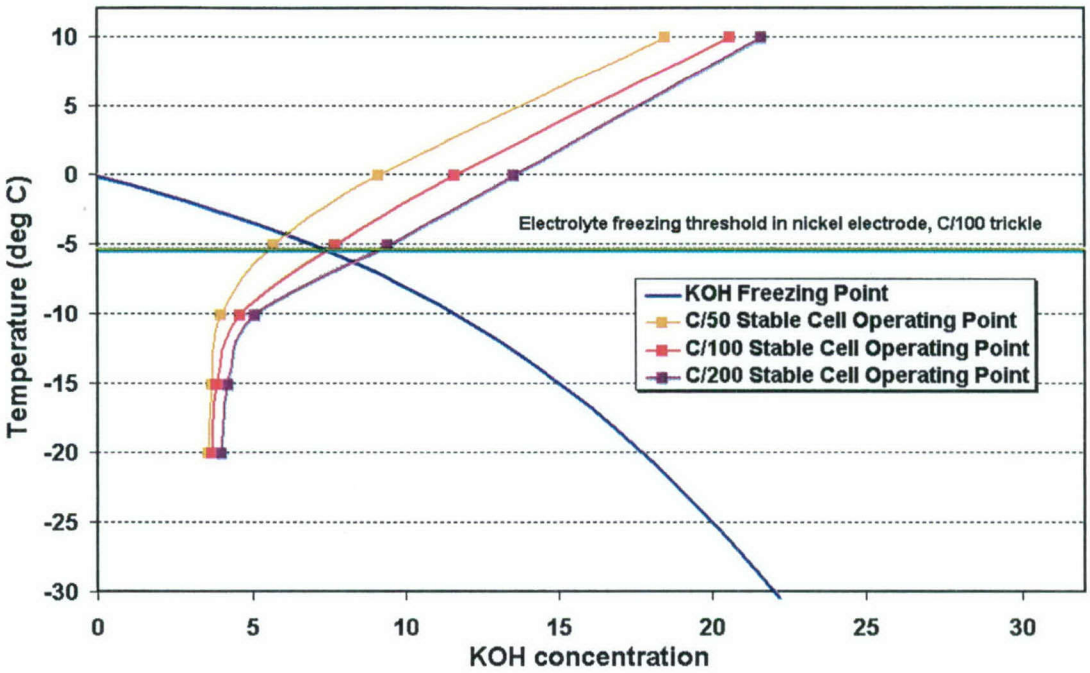

Figure 8. Stable cell electrolyte concentration during long-term trickle charge for different operating temperatures (3.0 g/Ah of 26% KOH). At the temperature where the operating curve for each trickle charge rate falls below the KOH freezing curve, it is likely that the cell will eventually experience problems associated with electrolyte freezing.

The results from these simulations can be summarized by plotting the KOH concentration that was attained in the stabilized cell after extended trickle charge, against the cell operating temperature. This provides an operating curve of cell KOH concentration over a range of temperature for each trickle charge rate, as indicated in Figure 8. Each of these curves is approximately linear down to about 5% KOH concentration, which is where the limit corresponding to 100% conversion to γ-NiOOH is approached. This limit is approached faster at higher trickle charge rates since higher overcharge rates favor the formation of the γ-NiOOH phase. If the freezing point curve of KOH electrolyte is superimposed on these operational curves, as has been done in Figure 8, the cell electrolyte is expected to freeze if the cell operating curve is below the freezing point curve at any specific temperature. As shown in Figure 8, the electrolyte can potentially freeze during long-term trickle charge at a C/100 rate if the cell temperature is below about –5°C. For a C/200 trickle charge rate, the freezing threshold appears to be about –6°C.

3.2 Model Results with 31% KOH Electrolyte

The results from the simulations done with the cell containing 3.5 g/Ah of 31% KOH electrolyte are summarized in Figures 9 through 11. Figure 9 shows the change in cell electrolyte concentration during the two cycles and the two-week trickle charge period when a C/100 trickle charge rate was used. For this model, complete conversion of all the active material into γ-NiOOH leaves the electrolyte at about a 15% concentration. Again, at the higher temperatures, it is significantly more difficult to form γ-NiOOH, thus the KOH concentration stabilizes at a level well above 15%. As the temperature is reduced to –10°C, it becomes possible to convert most of the active material to γ-NiOOH.

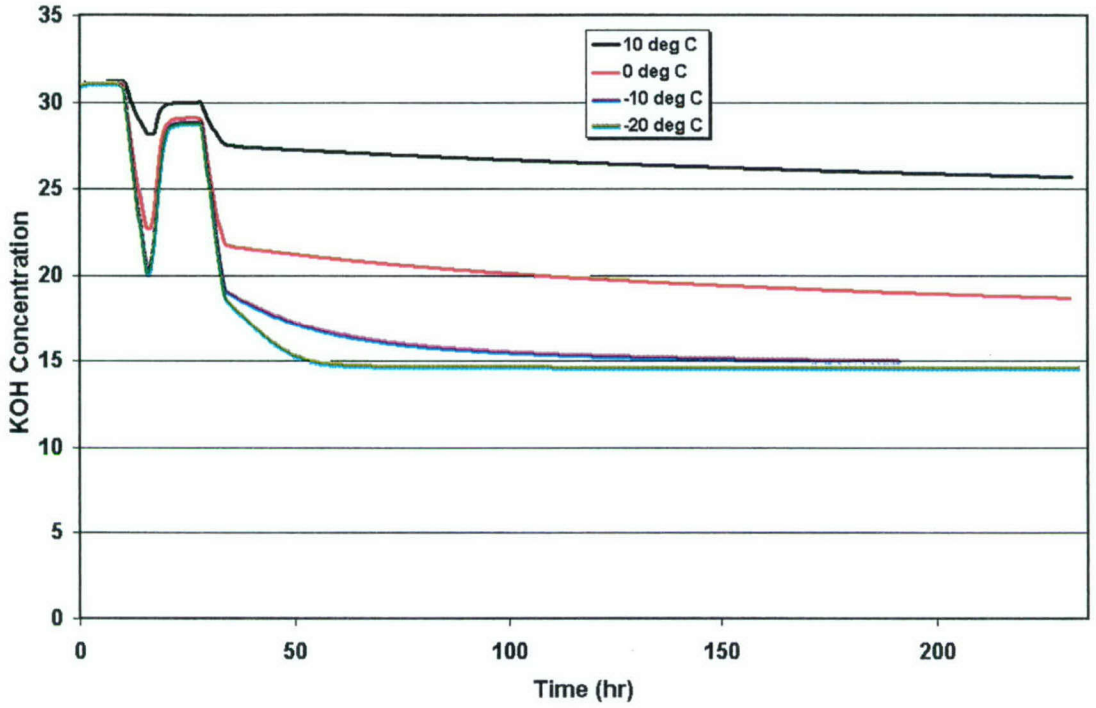

Figure 9. Concentration changes during simulations of a model cell initially containing 31% KOH, using a C/100 trickle charge rate. The concentration limit reached at about 15% corresponds to complete conversion of the active material to γ-NiOOH.

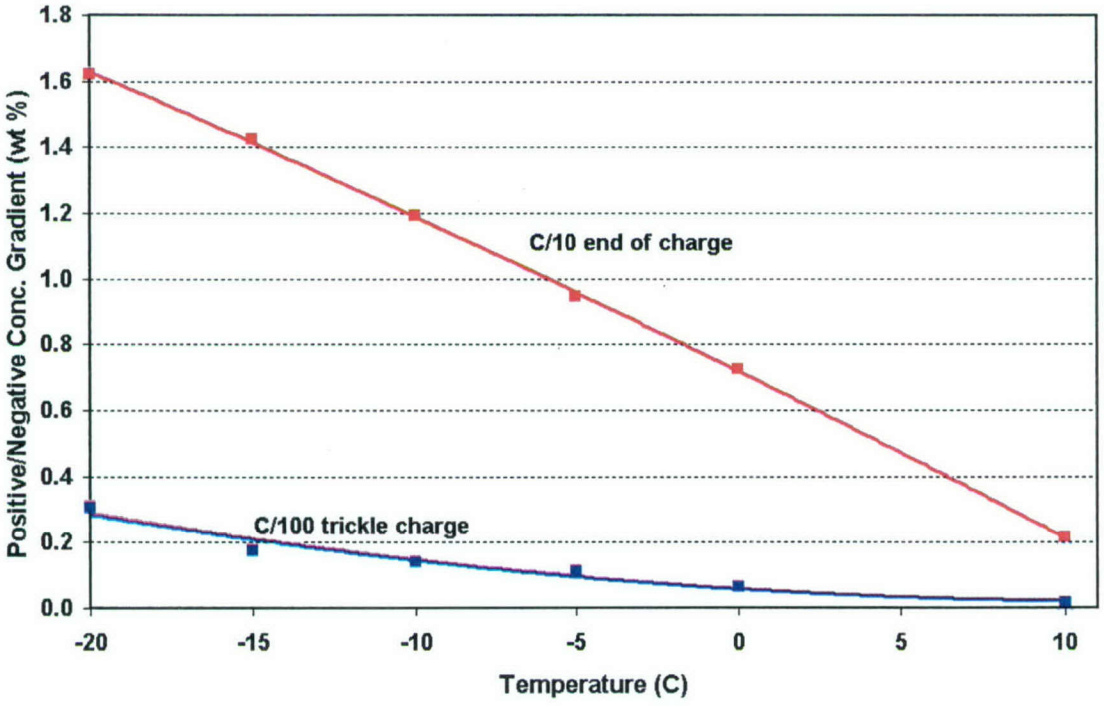

Figure 10. Worst-case electrolyte concentration gradient developed between the nickel and the hydrogen electrodes as a function of operating temperature, initially with 31% KOH.

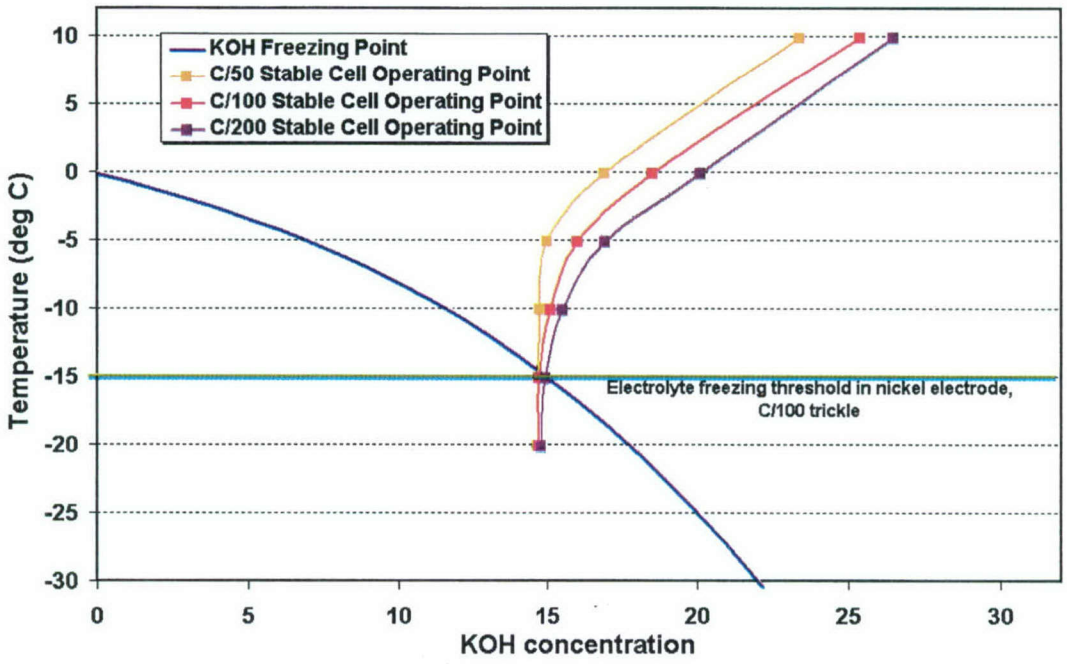

Figure 11. Stable cell electrolyte concentration during long-term trickle charge for different operating temperatures (3.5 g/Ah of 31% KOH). At the temperature where the operating curve for each trickle charge rate falls below the KOH freezing curve, it is likely that the cell will eventually experience problems associated with electrolyte freezing.

During the trickle charge period, less than a 0.1% concentration gradient was sustained between the nickel electrode and the hydrogen electrode at 0°C. At the end of the C/10 recharge, the concentration gradient between the electrodes was significantly greater. This observed concentration gradient at the end of the C/10 recharge and during the C/100 trickle charge are plotted in Figure 10. The concentration gradients increase as temperature falls, all the way down to –20°C, which was the lowest temperature at which this model was run. Since the model does not implicitly include the freezing of the KOH electrolyte, it continued to provide increasing concentration gradients in the electrolyte down to –20°C.

The results from these simulations can be summarized by plotting the KOH concentration that was attained in the stabilized cell after extended trickle charge against the cell operating temperature. This provides an operating curve of cell KOH concentration over a range of temperature for each trickle charge rate, as indicated in Figure 11. Each of these curves is approximately linear down to about 15% KOH concentration, which is where the limit corresponding to 100% conversion to γ-NiOOH is approached. This limit is approached faster at higher trickle charge rates since higher overcharge rates favor the formation of the γ-NiOOH phase. If the freezing point curve of KOH electrolyte is superimposed on these operational curves, as has been done in Figure 11, the cell electrolyte is expected to freeze if the cell operating curve is below the freezing point curve at any specific temperature. As shown in Figure 11, the electrolyte can potentially freeze during long-term trickle charge at a C/100 rate if the cell temperature is below about –15°C. For the case of 31% KOH electrolyte, the electrolyte freezing point is not sensitive to the trickle charge rate since by the time the electrolyte freezing point has been reached, essentially all the active material is in the γ-NiOOH phase regardless of the trickle rate.

4. Failure Mechanism in Real Cells

The mechanism described in this report for electrolyte freezing in operational cells is not generally regarded as causing catastrophic failures in real nickel-hydrogen cells. The typical analysis of electrolyte freezing is that it will cause high impedance in a cell, making it unable to undergo charge and discharge. However, when the cell is warmed up and the electrolyte thaws, it will regain the capability to charge and discharge normally. Here we analyze how an operating nickel-hydrogen cell would be expected to respond to electrolyte freezing, the potential consequences for cell degradation, and show that electrolyte freezing can significantly increase the likelihood of catastrophic cell failure.

In a real nickel-hydrogen cell, the thermal environment as well as the electrolyte concentration environment can vary significantly from one end of the electrode stack to the other. This variation can occur as a response to the thermal environment, overcharge within the cell, or previous cycling or operational history. For these reasons, as the temperature of a real cell is decreased it is likely that the electrolyte will initially freeze only at one end of the cell. If the cell is being cooled from its top end by heat pipes, the electrolyte at the top end of the stack will initially freeze. If the cell is being cooled from its bottom end as a result of being mounted to a cold base plate, the electrolyte at the bottom end of the stack will initially freeze.

As an example of the dynamics that would be expected once electrolyte freezing begins, we will examine a cell that is in trickle charge and is being cooled from its top end by a heat pipe assembly. If the cell temperature becomes too cold, the stack units at the top of the cell, being the coldest, will experience freezing of their electrolyte. This will effectively stop all electrochemistry in the electrodes where the electrolyte has frozen, thus stopping all further changes in their nickel electrode phase composition and electrolyte concentration.

The trickle charge current will then be forced to be completely carried by the remaining unfrozen stack units, thus increasing the trickle charge current density on the remaining active electrodes. The higher charge rate will result in the formation of more γ-NiOOH and a further drop in the electrolyte concentration in the remaining active stack units. The resulting reduction in electrolyte concentration will cause additional stack units to experience electrolyte freezing, which will stop all changes in their composition and force the current to be further concentrated towards the bottom of the cell.

This process will continue until eventually only the bottom-most stack units remain unfrozen. They will remain unfrozen because all the trickle charge current has been concentrated into them, and the resulting heat generation is sufficient to keep them from freezing. These bottom-most stack units will be exposed to extremely high overcharge rates as a result of all the cell current being concentrated into them. This will significantly increase the risk of damage and cell short-circuiting as a result of popping events. In addition, the extremely high levels of γ-NiOOH formation that will occur in the bottom-most nickel electrodes will cause tremendous expansion of the electrodes and the electrode stack. When this stack expansion is combined with that resulting from electrolyte freezing, it is pos-

sible that compressive damage to the stack components (negative electrodes and core) may occur. The cascade freezing process described above can thus lead to catastrophic cell failure in a period of time that is quite short compared to the normal lifetime of a nickel-hydrogen cell.

The mechanism described here can thus potentially lead to accelerated cell failure. This hypothetical failure mechanism can be validated by operating cells in trickle charge for long durations while looking for cell failure, or signs of stack damage in cell DPA. Such measurements could be made for cells containing differing amounts and concentrations of electrolyte, and exposing the cells to differing temperatures to find the temperature where failure occurs. In light of this mechanism, as well as the trend to operate nickel-hydrogen cells at lower temperatures that has occurred in the battery industry in recent years, understanding the temperature margin between where a cell is expected to operate and where it may fail is critically important.

5. Conclusions

A mechanism has been proposed that can potentially lead to rapid degradation and failure of nickel-hydrogen cells as a result of electrolyte freezing. It has been shown that there are chemical processes that can occur within the operating nickel-hydrogen cell that can raise the electrolyte freezing point in some cell designs up to the –5 to –10°C operational temperature range that cells can experience in some applications. The model that describes this failure mode suggests that the operational conditions where this failure mode is most likely to be seen is during long-term trickle charge at cold temperatures. It is recommended that nickel-hydrogen cell designs that are required to operate at temperatures well below 0°C should be evaluated for long-term degradation 10°C below their lowest expected operating temperature during extended trickle charge. This will assure that there is sufficient temperature margin to accommodate thermal variability between the individual cells in a battery power system.

References

1 (a) Zimmerman, A. H. and M. V. Quinzio, *Progress Towards Computer Simulation of NiH_2 Battery Performance Over Life*, Proc. of the 1994 NASA Battery Workshop, NASA Conf. Pub.3292, 177-184 (1994);

(b) Zimmerman, A. H., *Performance Model of a Nickel-hydrogen Cell*, ATR-93 (8363)-5, The Aerospace Corporation (15 October 1994).

LABORATORY OPERATIONS

The Aerospace Corporation functions as an "architect-engineer" for national security programs, specializing in advanced military space systems. The Corporation's Laboratory Operations supports the effective and timely development and operation of national security systems through scientific research and the application of advanced technology. Vital to the success of the Corporation is the technical staff's wide-ranging expertise and its ability to stay abreast of new technological developments and program support issues associated with rapidly evolving space systems. Contributing capabilities are provided by these individual organizations:

Electronics and Photonics Laboratory: Microelectronics, VLSI reliability, failure analysis, solid-state device physics, compound semiconductors, radiation effects, infrared and CCD detector devices, data storage and display technologies; lasers and electro-optics, solid-state laser design, micro-optics, optical communications, and fiber-optic sensors; atomic frequency standards, applied laser spectroscopy, laser chemistry, atmospheric propagation and beam control, LIDAR/LADAR remote sensing; solar cell and array testing and evaluation, battery electrochemistry, battery testing and evaluation.

Space Materials Laboratory: Evaluation and characterizations of new materials and processing techniques: metals, alloys, ceramics, polymers, thin films, and composites; development of advanced deposition processes; nondestructive evaluation, component failure analysis and reliability; structural mechanics, fracture mechanics, and stress corrosion; analysis and evaluation of materials at cryogenic and elevated temperatures; launch vehicle fluid mechanics, heat transfer and flight dynamics; aerothermodynamics; chemical and electric propulsion; environmental chemistry; combustion processes; space environment effects on materials, hardening and vulnerability assessment; contamination, thermal and structural control; lubrication and surface phenomena. Microelectromechanical systems (MEMS) for space applications; laser micromachining; laser-surface physical and chemical interactions; micropropulsion; micro- and nanosatellite mission analysis; intelligent microinstruments for monitoring space and launch system environments.

Space Science Applications Laboratory: Magnetospheric, auroral and cosmic-ray physics, wave-particle interactions, magnetospheric plasma waves; atmospheric and ionospheric physics, density and composition of the upper atmosphere, remote sensing using atmospheric radiation; solar physics, infrared astronomy, infrared signature analysis; infrared surveillance, imaging and remote sensing; multispectral and hyperspectral sensor development; data analysis and algorithm development; applications of multispectral and hyperspectral imagery to defense, civil space, commercial, and environmental missions; effects of solar activity, magnetic storms and nuclear explosions on the Earth's atmosphere, ionosphere and magnetosphere; effects of electromagnetic and particulate radiations on space systems; space instrumentation, design, fabrication and test; environmental chemistry, trace detection; atmospheric chemical reactions, atmospheric optics, light scattering, state-specific chemical reactions, and radiative signatures of missile plumes.